Spectrally selective surfaces of Co-pigmented anodic Al_2O_3

Blain, J.; LeBel, C.; Saint-Jacques, R. G.; Rheault, F.

Publisher's version / Version de l'éditeur:
https://doi.org/10.1063/1.335651
Journal of Applied Physics, 58, 1, pp. 490-494, 1985-07-01

Spectrally selective surfaces of Co-pigmented anodic Al_2O_3

J. Blain
Institut de Génie des Matériaux, Conseil National de Recherches du Canada, Boucherville, Québec, J4B 6Y4, Canada

C. LeBel, R. G. Saint-Jacques, and F. Rheault
INRS-Energie, Université du Québec, C. P. 1020, Varennes, Québec, J0L 2P0, Canada

(Received 12 October 1984; accepted for publication 5 March 1985)

The multilayer model of Al anodized selective surfaces has been revised by taking into account surface defects and incident angle of of illumination. This theory has been applied to Co-pigmented surfaces. Emphasis was put on extended experimental determination of all parameters used in the theory. With a detailed scanning and transmission electron microscope study of the structure, the size of the pores and their aerial density have been determined. Moreover, the surface roughness has been measured. This has permitted the calculation of the dielectric permeability for each layer. The permeabilities have then been used to compute spectral reflectance curves using the Bruggeman theory. Computer calculated reflectance curves based solely on experimental data agree well with experimental results for $\lambda \geqslant 2\,\mu$m. At shorter wavelengths, interference peaks that were predicted, but not observed, were minimized by considering surface roughness.

I. INTRODUCTION

Efficient solar energy collectors using photothermal conversion require spectrally selective surfaces.[1] Ideally, these surfaces absorb the solar radiations in the wavelength range of 0.4 to 2 or 3 μm, and they have zero emissivity for wavelengths $\geqslant 2$ or 3 μm. Granqvist *et al.*[2-3] have shown that Ni-pigmented Al_2O_3 formed by anodization of Al can have good spectral selectivity. The anodic film is known[4] to have an inhomogeneous microstructure made of columns oriented perpendicularly to the surface.

Granqvist *et al.*[3] have formulated a structural model of this anodic film. This model describes the anodic coating as four layers having different degrees of porosity and Ni content. However, the authors cited above did not study the microstructure in detail and particularly the size and the distribution of the pores. Moreover, they only evaluated the thickness of each layer. These parameters are needed in order to calculate the dielectric permeabilities which are used in the theoretical analysis. Therefore emphasis was put to experimentally measure the structure parameters in order to verify previous assumptions.

The purpose of this paper is twofold: firstly, to determine with greater accuracy the structure of the anodic film in order to calculate more precisely the dielectric permeability of each layer and improve the theoretical spectral reflectance curves. Secondly, by using Co-pigmented Al_2O_3, we provide a comparison with Ni-pigmented Al_2O_3. It then becomes possible to verify the layer model of Granqvist *et al.*[3] using a different pigmenting metal. Cobalt was chosen because it is a widely used pigment for anodized surfaces and because its electronic structure is close to that of nickel.

II. ANODIZATION AND COLORATION OF THE FILMS

The aluminum was anodized with dc current in dilute phosphoric acid to form a translucent oxide film. Three voltages where used (10, 14, and 18 V). The specimens obtained are referred to by H1, H3, and H5 in this paper. All films were then submitted to the same conditions of ac electrolysis in a bath containing cobalt sulfate. A dark coloration was achieved with metal precipitates at the bottom of the pores.

III. STRUCTURE

A. Scanning electron microscopy

Scanning electron microscopy (SEM) was used to study the morphology of the film perpendicularly to the interface. The samples were prepared from 1-cm^2 platelets cut from the anodized plates. The platelets were mechanically thinned from the metal side down to 100 μm with abrasive paper of grit 600. The brittle oxide (about 0.9 μm thick) was fractured by bending the metal over a very small radius. A 200-Å gold-palladium coating was deposited on the surface. The observations were made with a JEOL JSM-35CF SEM.

Figure 1 shows a fracture from which the total oxide thickness can be measured. The total thickness increases from 0.91 μm for H1, to 0.95 μm for H3, and to 1.77 μm for H5. The position of the four layers of the model[3] are shown on Fig. 1. The Al base metal is covered with a very thin Al_2O_3 layer (layer 4). The next layer (layer 3) is porous Al_2O_3

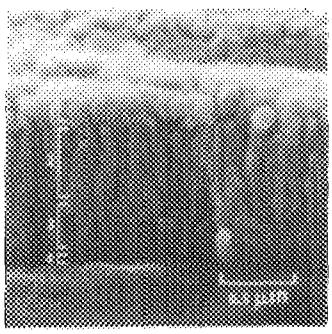

FIG. 1. Scanning electron micrograph showing a fractured coating of Co-pigmented anodic Al_2O_3. The numbers on the micrograph show the location of the four layers of the structural model of Granqvist *et al.* (see Ref. 3). These layers are described in Sec. III A.

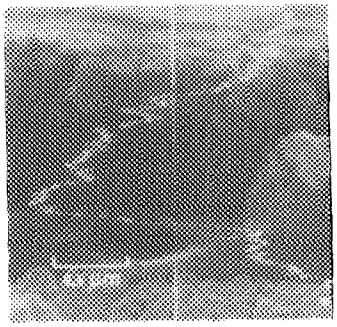

FIG. 2. X-ray line scan analysis showing the profile concentration of Co in Al_2O_3 film.

and contains Ni particles. The other layer (layer 2) is porous Al_2O_3 without Ni. The last layer (layer 1) represents the widening of the pores towards their opening. The thickness of layer 1 and its roughness can be measured (0.13, 0.05, and 0.10 μm). The thickness of layer 4 has been shown [4] to be of the order of 1 nm/V of anodization. These SEM observations confirm that the structure is elongated and porous. However, it is still not possible to evaluate the porosity from this high-resolution scanning micrography. The Co- particles are not visible, but an x-ray line analysis (Fig. 2) shows that the concentration of Co is maximum near the Al-Al_2O_3 interface.

B. Transmission electron microscopy

Transmission electron microscopy (TEM) was used to study the morphology of the film in a plane parallel to the interface. Samples were prepared from 100-μm-thick specimens. They were thinned from the metal sides with Ar bombardment (Ion Tech, Super Microlap). A uniform thinning rate was obtained by the continuous rotation of the disks during bombardment. The observations were made with a Philips EM 300 TEM.

Figure 3 shows the porous structure observed. The Co particles can be observed in some cases. From these micrographs we measured the diameter of the pores (or particles) and their aerial density. These values are given in Table I.

C. Atomic absorption analysis

We have measured to the Co concentration of the coatings with the aid of atomic absorption analysis. The concentrations in the specimens H1, H3, and H5 are, respectively, 0.57, 1.47, and 0.58 g/m^2. Since TEM observations showed that the pores were densely filled with Co, the thickness of layer 3 was derived from Co concentration, Co density, and

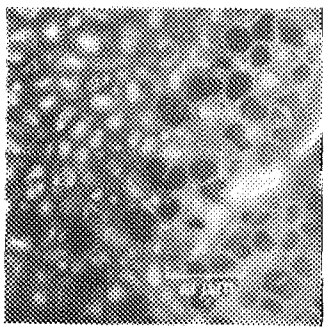

FIG. 3. Transmission electron micrograph showing the porous structure of the Al_2O_3 film. The pores which contain Co particles are black.

TABLE I. Average diameter of the pores (d) and average aerial density of the pores (D).

Sample	d (10^2 Å)	D (10^{10} cm^{-2})
H1	1.95	9.8
H3	3.15	4.3
H5	4.29	2.8

the porosity of the film. Having calculated[5] the thickness of layer 3 and measured by SEM the total thickness of the film and the thickness of layer 1, the thickness of layer 2 was derived. The measured or calculated values of thickness and porosity of each layer are given in Table II.

IV. OPTICAL PROPERTIES OF THE SURFACES

The specular reflectance of the pigmented surfaces was measured both in the infrared and visible regions. Measurements in the visible region were done at an incident angle of 20° while measurements in the infrared were done at an angle of 22°. For measurements in the visible region, a Cary model 17D spectrophotometer equipped with a specular reflectance accessory was used. For the infrared region, a Nicolet model 170X fast Fourier transform spectrophotometer also equipped for specular reflectance was used.

All measurements were done relatively to an aluminized control mirror with a reflectance of 93%. The spectra covered by each spectrophotometer overlapped in the 1.30–2.60-μm region. In all cases, measurements from both machines agreed very well so than no correction had to be used to make the measurements coincide.

The angle of aperture of the infrared specular reflectance accessory was 10°, and this figure was used in the computer model developed to predict the reflectance of our films.

V. THEORY

In order to compute the spectral selectivity of the film, it is necessary to know the dielectric permeability of layer 3 which contains the Co particles. The averaged permeability of the layer can be obtained with "effective medium theories".[6–8] In agreement with previous work[3] using Ni we found

TABLE II. Thickness and porosity of each layer.

		Samples		
		H1	H3	H5
Thickness (μm)	Layer 1	0.13	0.05	0.10
	Layer 2	0.55	0.40	0.89
	Layer 3	0.22	0.49	0.16
	Layer 4	0.01	0.01	0.02
Porosity (%)	Layer 1	58	68	82
	Layer 2	29	34	41
	Layer 3	29	34	41
	Layer 4	0	0	0

the Bruggeman theory[6] to be the more accurate for our system. The effective dielectric permeability $\bar{\epsilon}^{Br}$ is given by[6]

$$\bar{\epsilon}^{Br} = \epsilon_m\left(1 - f + \frac{1}{3}f\alpha\right)/\left(1 - f - \frac{2}{3}f\alpha\right)$$

with $\alpha = (\epsilon - \bar{\epsilon}^{Br})/[\bar{\epsilon}^{Br} + 1/3(\epsilon - \bar{\epsilon}^{Br})]$, where ϵ_m is the permeability of the medium Al_2O_3, f is the filling factor, and ϵ is the permeability of the Co particles. This formula can be generalized for nonspherical particles.

In the case of a film constituted of four layers of thickness t_i, the total reflectivity is given by[9]

$$R = \left|\frac{AN_0 - C + (BN_0 - D)N_s}{AN_0 + C + (BN_0 + D)N_s}\right|^2,$$

where N_s is the refraction index of the metallic substrate, N_0 is the refraction index of air (~ 1), and A, B, C, and D are the elements of the transfer matrix M:

$$M = \prod_{i=1}^{4} M_i = \begin{pmatrix} A & B \\ C & D \end{pmatrix},$$

$$M_i = \begin{pmatrix} \cos\xi_i & -(i/P_i)\sin\xi_i \\ -iP_i\sin\xi_i & \cos\xi_i \end{pmatrix},$$

$$\xi_i = 2\pi\frac{N_i t_i}{\lambda}\cos\theta_i,$$

$$P_i = N_i\cos\theta_i,$$

θ_i = angle of propagation of incident light in layer i.

The refractive indices $N_i = \epsilon_i^{1/2}$ for each layer of our films were calculated from tabulated values[10–15] of dielectric permeabilities of Al_2O_3 and Co. For each layer the Bruggeman theory was used to derive the effective permeability.

In this paper we have modified R in order to consider surface defects and the spectrophotometer aperture angle. This modification has been done by using the following formula[16]:

$$R_s = R\left\{\exp - \left(\frac{4\pi n_0\sigma}{\lambda}\right)^2 + \left[1 - \exp - \left(\frac{4\pi n_0\sigma}{\lambda}\right)^2\right] \times \left[1 - \exp - 2\left(\frac{\pi\sigma\alpha}{m\lambda}\right)^2\right]\right\}$$

where R_s = reflectivity of the rugged surface,
R = reflectivity of the smooth surface,
σ = RMS height of defects,
m = RMS slope of defects,
α = spectrophotometer aperture angle,
n_0 = index of ambiant medium.

This is a different approach from previous work[3] in which roughness was introduced as a nonuniformity in the evaluated thickness of each layer. Since in our case such a variation in thickness was impossible to measure, we only considered surface roughness which we could precisely measure.

VI. DISCUSSION

From the results given in Table II and from the simulation program of selective surfaces, a series of curves of R vs λ have been obtained.

A. Selectivity of the various layers

Figure 4 shows the calculated reflectivity of the various layers composing sample H1 as well as the experimentally measured reflectivity of H1. Layer 3 (containing Co) shows a good selectivity, although the reflectivity is high for short wavelength λ. When the porous layers are added, the short λ reflectivity decreases. Layers 1 and 2 have an almost identical effect. However, in the visible region, interference peaks are observed due to the multilayer arrangement layers. Layer 4 has negligible effect.

B. Surface defects

In general, dispersion of visible light by surface defects is highly dependent on λ. This effect is clearly shown by comparing the calculated and experimental results. In fact, the interference peaks shown by the experimental results are much weaker than the ones predicted by a theory for smooth surfaces. Hence by adding in the program a factor that takes into account the half-height size and angle of the surface defect of layer 1, it is possible to obtain a much better agreement as shown in Fig. 5 for 0.05-μm surface defects.

C. Shape of particles

For particles elongated along the pores or flattened particles (i.e., prolate or oblate spheroids), the Bruggeman theory is modified by the addition of a depolarization factor L. In the case of prolate spheroids[17]:

$$L = \frac{e_p^{-2}}{2} - \frac{1}{4}(e_p^{-3} - e_p^{-1})\ln\left(\frac{1 + e_p}{1 - e_p}\right),$$

with $e_p = (1 - c^2/a^2)^{1/2}$ and a and c are major and minor axes. In the Bruggeman equation, the parameter α is then modified:

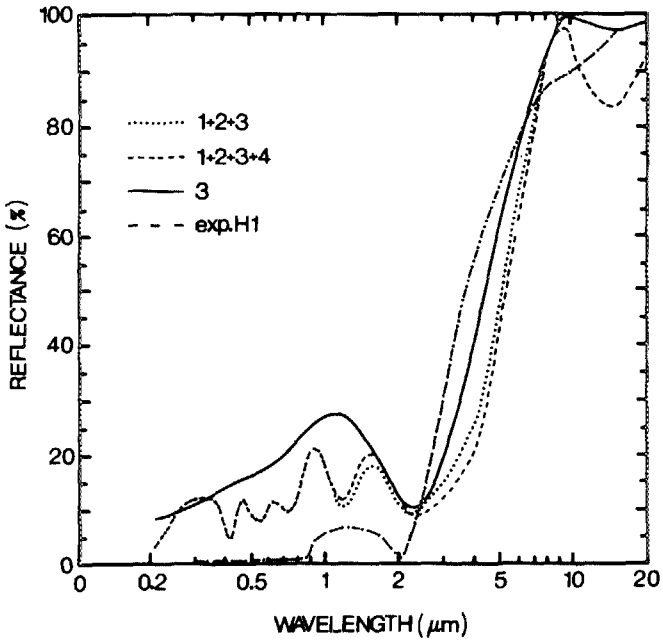

FIG. 4. Spectral reflectance for Al_2O_3 films containing 0.57 g/m^2 of Co. The numbers in the curve designation refer to the layers of the structural model illustrated in Fig. 1. The Bruggeman formalism was used.

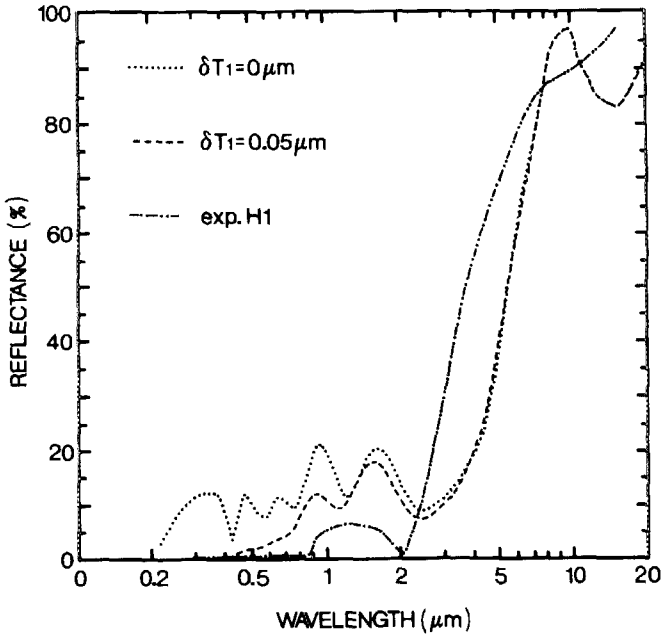

FIG. 5. Spectral reflectance for Al_2O_3 films containing 0.57 g/m^2 of Co. A theoretical curve representing a smooth surface is shown as well as a theoretical curve where layer 1 has measured surface irregularities of 0.05 μm.

$$\alpha = \frac{(\epsilon - \bar{\epsilon}^{Br})}{[\bar{\epsilon}^{Br} + L(\epsilon - \bar{\epsilon}^{Br})]}.$$

Figure 6 shows the effect of the variation of L on the layer 3. From $L = 0.3$ to 0.5 the value of the critical wavelength λ_c (50% reflectance) is lowered. However, below 0.3, λ_c does not increase as expected but diminishes. This may be due to the fact the oblate spheroids are randomly oriented in the pores instead of being normal to the surface.

Moreover, for $L = 0.4$ the theoretical λ_c is close to the experimental one. Hence the particles seem to have a tendency to be slightly elongated along the pores.

Figure 7 shows in the case of sample H5 the experimental curve, a theoretical curve for spherical particles ($L = 1/3$) and smooth surface ($\delta T_1 = 0$) and a theoretical curve for $L = 0.4$ and $\delta T_1 = 0.05\,\mu$m. The fit is better for $L = 0.4$ and $\delta T_1 = 0.05\,\mu$m. A similar situation exists for samples H1 and H3.

D. Short wavelength discrepancy

Figure 7 shows that, even when particle elongation and surface roughness are included in the model, there still exists a difference between theoretical and experimental results. While the model predicts interference peaks due to multiple reflections in the layers, none are observed. This difference leads to a better than predicted selectivity of our films, due to enhance absorption at shorter wavelengths.

This difference is a direct result of the multilayer model that we use. A much better fit could be obtained at shorter wavelengths if the model were to take into account the nonuniform thickness of the layers and include a gradual transition in permittivity from one layer to the next. Using numerical simulations, Trotter and Sievers[18] have shown that smoothly graded films can show no interference peaks at short wavelengths while still being very selective.

However, since no experimental data on the transition profile from one layer to another is currently available for anodized aluminum surfaces, a simpler model had to be used. Work is now under way to try to measure the exact permittivity profile of our films and will be reported along with a revised model in a subsequent paper.

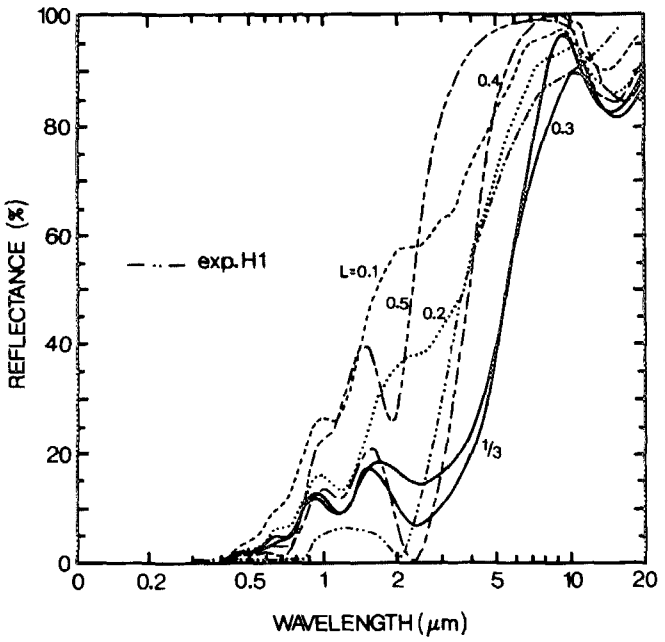

FIG. 6. Spectral reflectance for Al_2O_3 films containing 0.57 g/m^2 of Co. The theoretical curves were obtained for spheroidal particles (layer 3) with symmetry axis perpendicular to the film surface and with shapes governed by the shown depolarization factors. The curve with $L = 1/3$, i.e., for spherical particles, is identical with the dotted curve in Fig. 5.

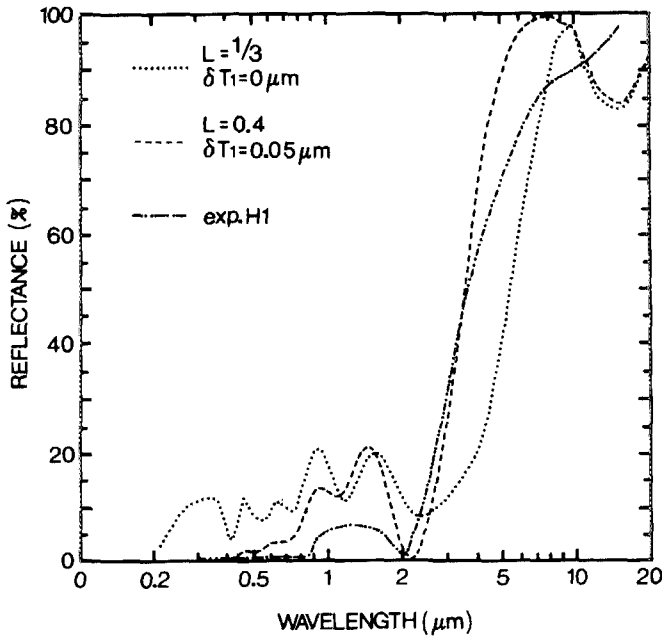

FIG. 7. Spectral reflectance for Al_2O_3 films containing 0.57 g/m^2 of Co. One theoretical curve is for a smooth surface and spherical particles. The other is for surface having the indicated measure roughness and for layer 3 containing Co particles elongated along the pores.

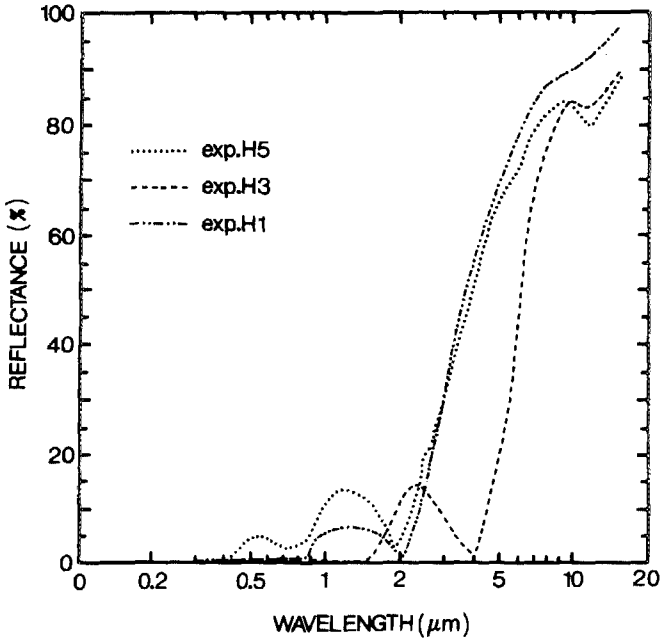

FIG. 8. Spectral reflectance for Al_2O_3 films containing the following Co concentrations: 0.57 g/m^2 (H1), 1.47 g/m^2 (H3), and 0.58 g/m^2 (H5).

E. Comparison between the samples

When the three experimental curves are compared (Fig. 8), one notices that H1 and H5 have the same λ_c ($\sim 4\ \mu$m) whereas H3 has a higher λ_c ($\sim 6\ \mu$m). This is explained by the larger quantity of Co present in H3.

VII. CONCLUSION

This work reports results of a detailed experimental and theoretical study on selective surfaces produced by anodization and Co coloration of Al.

From the measured structure characteristics of the oxide films using the Bruggeman theory, the average dielectric permeabilities of various layers of the films have been computed. The theoretical results for smooth surfaces and layers of constant thickness agree very well with experimental results at medium and large λ (2–20 μm). However, an important discrepancy is observed at short λ. Theoretical results show important interference peaks whose experimental amplitude is much less important. The agreement between theory and experiment is improved by adding to the model factors that account for the nonsphericity of the Co particles, for surface roughness, and for the incident angle of illumination. A better agreement could be obtained by using a graded film model. However, before using such a model, the exact permittivity profile of the film needs to be determined.

From a practical point of view for solar applications, these selective surfaces have shown a very high selectivity ($\alpha = 94\%$ and $e = 10\%$). Moreover, the Co concentration is a sensitive mean of controlling the critical wavelength.

ACKNOWLEDGMENTS

This work has been supported by the Ministry of Education of Québec and the Natural Sciences and Engineering Research Council of Canada. The authors would like to express their appreciation to G. Veilleux for his advice in TEM sample preparation and to J. Massounave for his help in high-resolution SEM.

[1] B. O. Seraphim, *Solar Energy Conversion: Solid State Physics Aspects, Topics in Applied Physics*, Vol. 31, edited by B. O. Seraphim (Springer, Berlin, Heidelberg, 1979), p. 5.
[2] C. G. Grangvist, Å. Anderson, and O. Hunderi, Appl. Phys. Lett. **35**, 268 (1979).
[3] Å. Anderson, O. Hunderi, and C. G. Granqvist, J. Appl. Phys. **51**, 754 (1980).
[4] S. Wernick and R. Pinner, *The Surface Treatment and Finishing of Aluminum and its Alloys*, 4th ed. (Draper, Teddington, U.K., 1972).
[5] C. LeBel, M. Sc. Thesis, INRS-Energie, Université du Québec, 1984.
[6] D. A. G. Bruggeman, Ann. Phys. (Leipzig) **24**, 636 (1935).
[7] J. C. M. Garnett, Philos. Trans. R. Soc. (London) **203**, 385 (1904); **205**, 237 (1906).
[8] G. Mie, Ann. Phys. (Leipzig) **25**, 377 (1908).
[9] M. Born and E. Wolf, *Principles of Optics* (Pergamon, Oxford, 1965), p. 633.
[10] A. P. Lenham and D. M. Treherne, J. Opt. Soc. Am. **56**, 1137 (1966).
[11] P. B. Johnson and R. N. Christy, Phys. Rev. B **9**, 5056 (1974).
[12] A. P. Lenham and D. M. Treherne, in *Optical Properties and Electronic Structure of Metal Alloys*, edited by F. Abelès (North-Holland, Amsterdam, 1966), p. 196.
[13] A. G. Mathewson and H. P. Meyers, Phys. Scr. **4**, 291 (1971).
[14] H. Ehrenreich, H. R. Philipp, and B. Segall, Phys. Rev. **132**, 1918 (1963).
[15] T. S. Erikson, A. Hjortsberg, G. A. Niklasson, and C. G. Granqvist, Appl. Opt. **20**, 2742 (1981).
[16] C. L. Nagendra and G. K. M. Thutupalli, Appl. Opt. **20**, 2747 (1981).
[17] Landau and Lifchitz, *Electrodynamique des Milieux Continus* (Editions Mir, Moscou, 1969), p. 36.
[18] D. M. Trotter and A. J. Sievers, Appl. Opt. **19**, 711 (1980).